

Electronic Supplementary Information

Reductive Stress Imaging in the Endoplasmic Reticulum by Using Living Cells and Zebrafish

Huawei Niu,^a Yongru Zhang,^a Fangfang Zhao,^a Saijun Mo,^c Wenbo Cao,^c Yong Ye^{*,a} and Yufen Zhao^{a,b}

^a College of Chemistry and Molecular Engineering, Zhengzhou University, Zhengzhou 450001, P.R. China. E-mail: yeyong03@tsinghua.org.cn

^b Ningbo Univ, Inst Drug Discovery Technol, Ningbo 450052, Zhejiang, P. R China.

^c School of Basic Medical Science, Zhengzhou University, Zhengzhou 450001, China

Table of contents:

Experimental

Fig. S1 Structure characterization of compound 2

Fig. S2 Structure characterization of compound 3

Fig. S3 Structure characterization of probe NPCC

Fig. S4 The relationship between the emission intensity of NPCC and different pH medium before or after treated with Cys or GSH

Fig. S5 UV-vis absorption spectra and fluorescence spectra changes of probe NPCC in the presence of Cys, GSH and ClO⁻

Fig. S6 Absorption and emission spectra of NPCC toward Cys, GSH and other respective species

Fig. S7 Fluorescence spectra of NPCC toward Cys, GSH and other analytes

Fig. S8 Time-dependent fluorescence of NPCC before and after treated with Cys or GSH

Fig. S9 Emission changes of NPCC with GSH and Cys at the prescribed time (0-22.5 min)

Fig. S10 Time-dependent fluorescence of NPCC/Cys and NPCC/GSH before and after treated with ClO⁻

Fig. S11 Absorption and emission spectra of NPCC/GSH toward ClO⁻ and other analytes

Fig. S12 The emission ratio (I_{412}/I_{514}) of NPCC/GSH toward different 30 equiv. of analytes

Fig. S13 The changes of the emission ratio (I_{412}/I_{514}) of NPCC/Cys and NPCC/GSH in different pH

Fig. S14 Sensing mechanism of NPCC toward Cys, GSH and ClO⁻

Fig. S15 Different probe NPCC concentrations were tested in EC1 cells for toxicity

Fig. S16 Imaging of NPCC for detecting endogenous and exogenous Cys, GSH and ClO⁻ in EC1 cells

Fig. S17 TP imaging of Cys, GSH and ClO⁻ in EC1 cells

Fig. S18 Imaging of cancer cells and normal cells

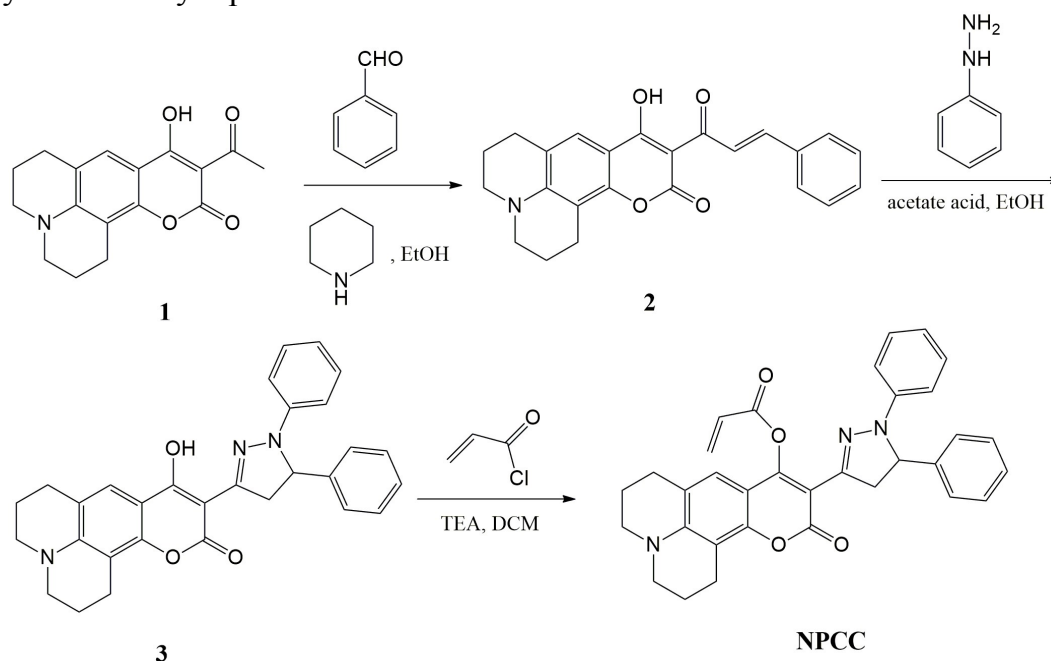
Experimental

Materials and chemicals

Acryloyl chloride, phenylhydrazine, triethylamine, and benzaldehyde were gained from Shanghai Aladdin Bio-Chem Technology Co., Ltd. Dichloromethane, ethanol, and acetic acid were charged from Tianjin Kemiou Chemical Reagent Co., Ltd. ER-Tracker Red (BODIPY® TR Glibenclamide) was purchased from Yeasen Biotech Co., Ltd. Dichloromethane was dried over calcium hydride, and then refluxed to give anhydrous dichloromethane. The water used throughout the experiment was deionized water.

Instrumentation and equipment

Absorption spectra were accurately recorded on a UV-2102 double-beam UV/VIS spectrometer, Perkin Elmer. Fluorescence spectra were performed on an F-4500 FL Spectrophotometer. The pH was performed on a model pHs-3C meter (Shanghai, China). NMR spectra were evaluated using a Bruker DTX-400 spectrometer. ESI mass spectra were measured on an HPLC Q-Exactive HR-MS spectrometer (Thermo, USA). Cells and zebrafish were imaged on a LEICA TCS SP8 laser scanning confocal microscope. Compound 1 was synthesized by reported methods.^{S1}



Scheme S1 Synthesis procedure of NPCC.

Synthesis

Synthesis of compound 2. Compound 1 (897 mg, 3 mmol) and benzaldehyde (334 mg, 3.15 mmol) were added into 25 mL EtOH followed by the addition of six drops of piperidine. This solution was then refluxed for 14 h. After completion of the reaction, it resulted in the formation of a precipitate,

which was isolated by filtrations, washed with frozen ethanol, and dried under vacuum. Compound 2 was obtained as a red solid (896.4 mg, yield 77.2%). ¹H NMR (400 MHz, CDCl₃, ppm): 1.92-1.99 (m, 4H), 2.76-2.85 (m, 4H), 3.29-3.32 (m, 4H), 7.42 (m, 4H), 7.70 (m, 2H), 7.94 (d, 1 H, *J* = 15.8 Hz), 8.46 (d, 1 H, *J* = 15.8 Hz); ¹³C NMR (100 MHz, CDCl₃, ppm): δ = 20.14, 20.25, 21.22, 27.48, 49.82, 50.25, 98.06, 103.11, 105.36, 118.70, 122.75, 124.07, 128.88, 128.96, 130.55, 135.27, 144.41, 149.38, 152.26, 161.51, 179.36, 191.56; HR-MS: *m/z* [M+H]⁺ calcd for [C₂₄H₂₁NO₄+H]⁺: 388.1543. Found: 388.1545.

Synthesis of compound 3. Compound 2 (194 mg, 0.5 mmol), phenylhydrazine (0.162 g, 1.5 mmol) and acetic acid (0.5 mL) were added into 25 mL EtOH. The reaction mixture was refluxed for 4 h. After completion of the reaction, it resulted in the formation of a precipitate, which was isolated by filtration, washed with frozen ethanol, and dried under vacuum. Product 3 was obtained as a yellow solid (233 mg, yield 97.7%). ¹H NMR (400 MHz, CDCl₃, ppm): 2.00 (m, 4H), 2.82-2.90 (m, 4H), 3.30-3.31 (m, 4H), 3.53-3.60 (m, 1H), 4.21-4.29 (m, 1H), 5.09-5.15 (m, 1H), 6.85 (t, 1H, *J* = 31.4 Hz), 6.93 (d, 2H, *J* = 17.4 Hz), 7.23 (t, 2 H, *J* = 21.4 Hz), 7.30 (s, 1 H), 7.36-7.42 (m, 5 H), 13.85 (s, 1 H); ¹³C NMR (100 MHz, CDCl₃, ppm): δ = 20.38, 20.51, 21.48, 27.67, 46.89, 49.65, 50.09, 63.43, 91.85, 103.15, 105.84, 113.15, 118.51, 119.56, 121.05, 125.99, 127.59, 129.10, 129.47, 142.27, 144.65, 147.12, 150.76, 151.57, 162.10, 167.36; HR-MS: *m/z* [M+H]⁺ calcd for [C₃₀H₂₁N₃O₃+H]⁺: 478.2125. Found: 478.2115.

Synthesis of probe NPCC. Acryloyl chloride (90.5 mg, 0.225 mmol) in dichloromethane (DCM, 5 mL) was added dropwise at 0°C to a stirred solution of compound 3 (83.5 mg, 0.175 mmol) and Et₃N (25 mg, 0.25 mmol) in DCM (10 mL). The reaction mixture was allowed to stir at room temperature for 4 h. After the reaction was completed, the mixture was washed with brine (10 mL×3) and dried over MgSO₄. The combined organic layers were evaporated under reduced pressure. The crude product was purified by column chromatography on silica gel with petroleum ether and DCM (1/1, v/v) to afford NPCC as a pale saffron yellow solid (60 mg, yield 65 %). ¹H NMR (400 MHz, CDCl₃, ppm): 2.00 (m, 4H), 2.82-2.90 (m, 4H), 3.30-3.31 (m, 4H), 3.53-3.60 (m, 1H), 4.21-4.29 (m, 1H), 5.09-5.15 (m, 1H), 6.85 (t, 1H, *J* = 31.4 Hz), 6.93 (d, 2H, *J* = 17.4 Hz), 7.23 (t, 2 H, *J* = 21.4 Hz), 7.30 (s, 1 H), 7.36-7.42 (m, 5 H), 13.85 (s, 1 H); ¹³C NMR (100 MHz, CDCl₃, ppm): δ = 20.38, 20.51, 21.48, 27.67, 46.89, 49.65, 50.09, 63.43, 91.85, 103.15, 105.84, 113.15, 118.51, 119.56, 121.05, 125.99, 127.59, 129.10, 129.47, 142.27, 144.65, 147.12, 150.76, 151.57, 162.10, 167.36; HR-MS: *m/z* [M+H]⁺ calcd for [C₃₃H₂₉N₃O₄+H]⁺: 532.2231. Found: 532.2222.

Detection limits calculation

The detection limits (DLs) of Cys, GSH and ClO⁻ were calculated by the following equation 1

$$DL = \sigma/K \quad \text{equation 1}$$

Where σ is the standard deviation of blank measurement, K is the slope of the calibration curve.

Three good linear relations (for detecting Cys, $R^2 = 0.98488$; for detecting GSH, $R^2 = 0.98770$; for detecting HOCl, $R^2 = 0.98222$) were investigated in the range from 0 to 0.9 equiv., 0 to 0.9 equiv. and 2 to 9 equiv. respectively. They had low DLs of 8.95 nM, 4.26 nM, and 0.43 μ M, respectively.

Cellular imaging

All cells were cultured in Dulbecco's modified Eagle's medium (DMEM) replenished with 10% fetal bovine serum at 37 °C.

Cytotoxicity assay. Cytotoxicity assay was implemented by using Cell Counting Kit-8 (CCK-8) according to our previously reported.^{S2} The concentrations of NPCC were 0, 2.5 μ M, 5 μ M, 10 μ M, 15 μ M, and 20 μ M, respectively.

Imaging of exogenous Cys, GSH and HOCl in EC1 cells. EC1 cells were treated with N-ethylmaleimide (NEM, scavenger of thiol) ^{S3} for 0.5 h as a control experiment, followed by treatment with NPCC for 0.5 h. Next, we used NEM to avoid possible mutual interference from Cys and GSH, followed by adding Cys and GSH for 0.5 h, respectively, and then added NPCC for 0.5 h. Finally, the above cells were separately incubated with ClO⁻ for 0.5 h.

Imaging of TP fluorescence. NPCC were incubated with Cys and GSH for 0.5 h, respectively, and then imaged with 780 nm excitation (λ_{em} = 492–532 nm).

Distinguishing between normal cells and cancer cells. NPCC were separately incubated with cancer cells (EC1 cells and Hela cells) and normal cells (L929 cells and EC) for 0.5 h, respectively, and then imaged in the same conditions.

Determining co-localization experiment of NPCC in the ER. GSH (100 μ M) was incubated with EC1 cells for 0.5 h, followed by treatment with 10 μ M of NPCC and 1 μ M of ER-Tracker Red (BODIPY[®] TR Glibenclamide) for 0.5 h. The overlap coefficient of the ER positioning experiment was 0.8624. Conditions: for green channel, λ_{ex} = 440 nm, λ_{em} = 492–532 nm; for red channel, λ_{ex} = 587 nm.

Imaging of EC1 cells under reductive stress over time

NPCC was incubated with EC1 cells for 0.5 h, followed by treatment with GSH (1 mM), and then imaged. The green channel of fluorescence intensity was obtained in the range of 492–532 nm (λ_{ex} = 440 nm), the blue channel of fluorescence intensity was obtained in the range of 392–432 nm (λ_{ex} = 380 nm).

Zebrafish confocal fluorescence imaging

Wild zebrafish were gained from Shanghai Fish-bio Co., Ltd. Zebrafish were reared in E3 media at 28 °C. The 2-day-old zebrafish were incubated with NPCC (10 μ M) for 1 h, followed by treatment with GSH (5 mM), and then

imaged. Zebrafish were imaged on a Zeiss LSM 880 confocal microscope using a 10×objective. The green channel of fluorescence intensity was obtained in the range of 492–532 nm ($\lambda_{\text{ex}} = 440$ nm), the blue channel of fluorescence intensity was obtained in the range of 392–432 nm ($\lambda_{\text{ex}} = 380$ nm).

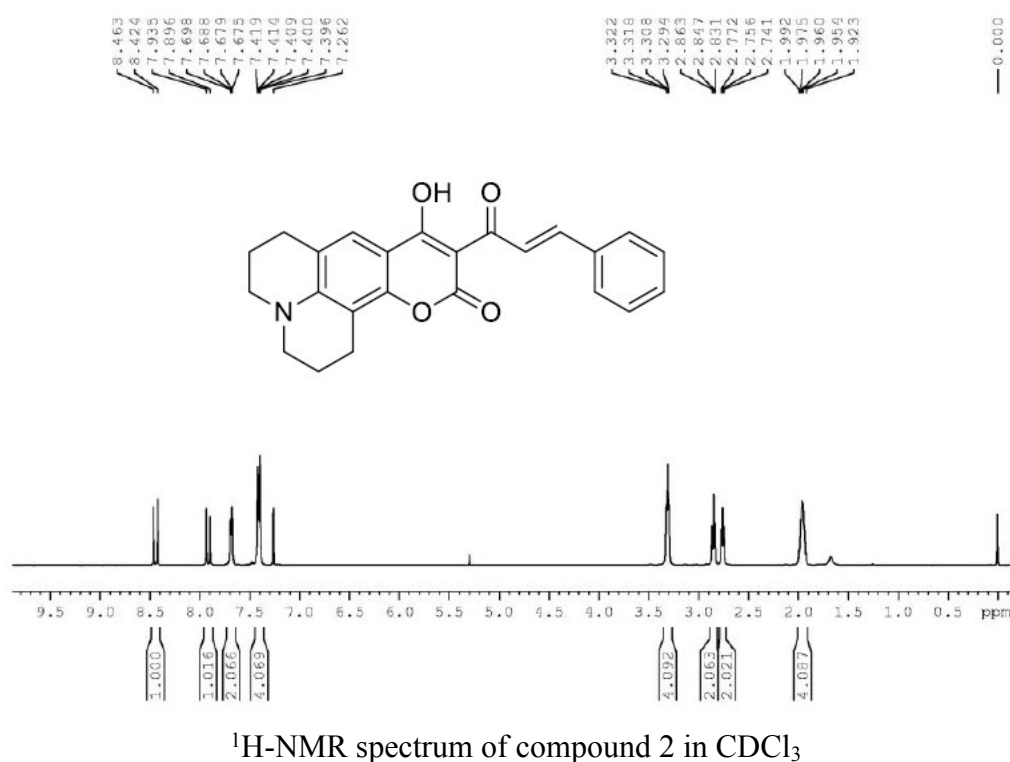
Live subject statement:

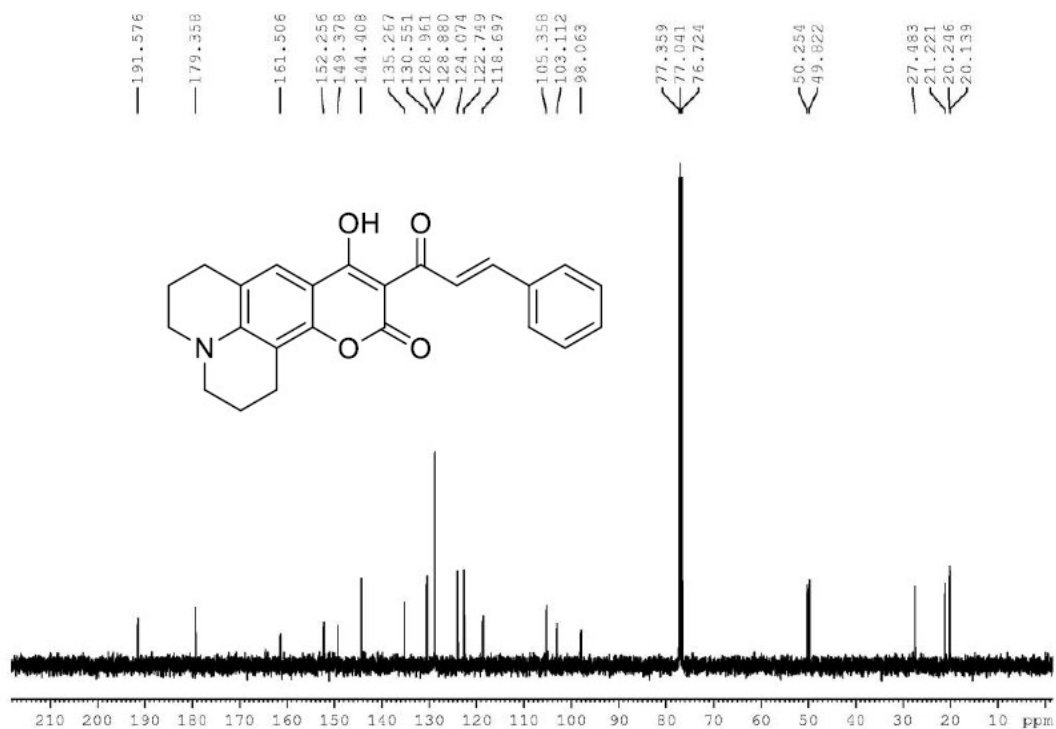
Procedures involving animals and their care were conducted in conformity with the guidelines of the Use and Care of Laboratory Animals of National Institutes of Health (NIH Pub. No. 85-23, revised 1996). Ethics committee approval was obtained from the Animal Ethical Experimentation Committee of The First Affiliated Hospital of Zhengzhou University, China.

References

- S1 A. Fedorov, A. Nyuchev, K. Schegravin, M. Lopatin, V. Fokin and I. Beletskaya, *Synthesis*, 2014, **46**, 3239–3248.
- S2 X. Yang, W. Liu, J. Tang, P. Li, H. Weng, Y. Ye, M. Xian, B. Tang and Y. Zhao, *Chem. Commun.*, 2018, **54**, 11387–11390
- S3 S. Yang, C. Guo, Y. Li, J. Guo, J. Xiao, Z. Qing, J. Li and R. Yang, *ACS. Sens.*, 2018, **3**, 2415–2422.

Fig. S1 Structure characterization of compound 2





¹³C-NMR spectrum of compound 2 in CDCl₃

HR-MS spectrum of compound 2

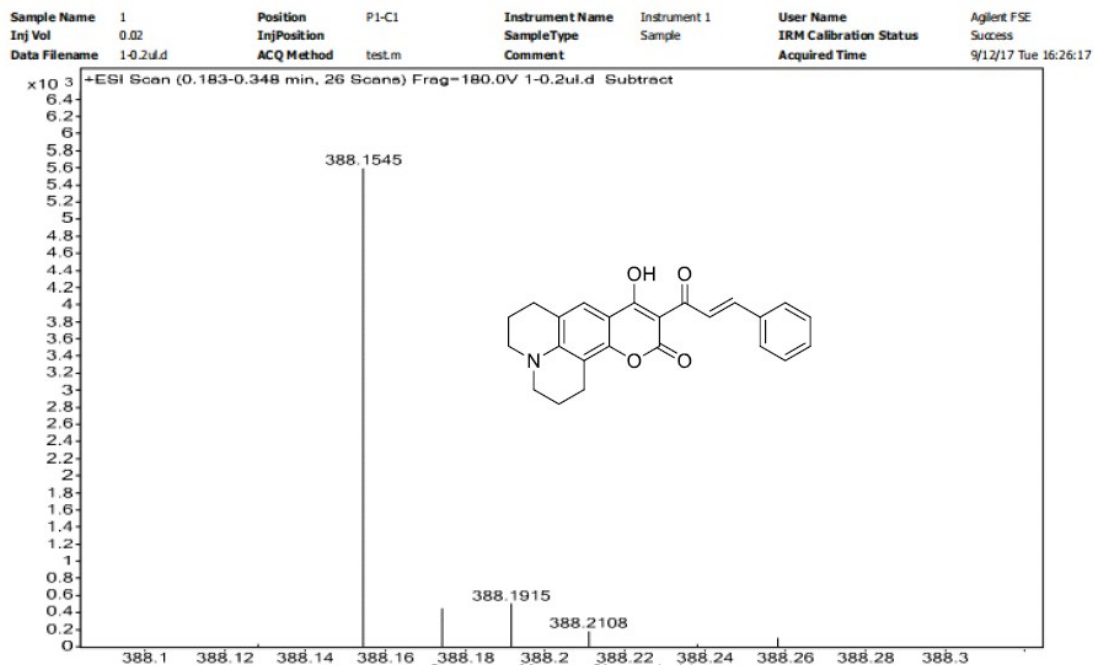
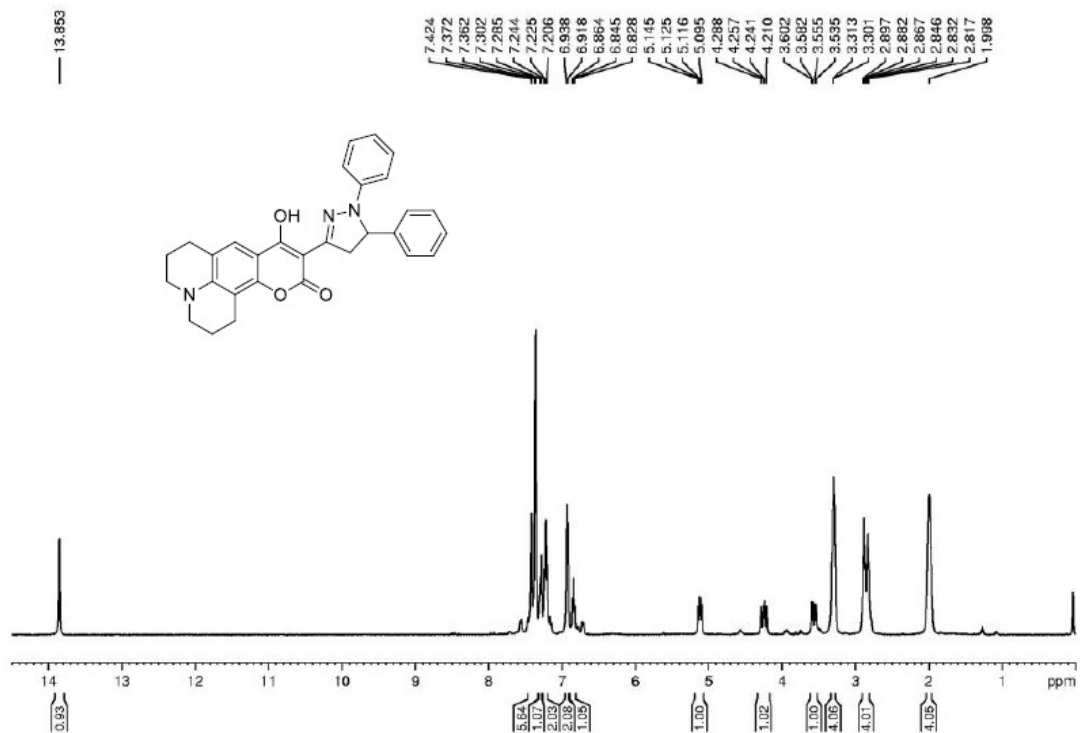
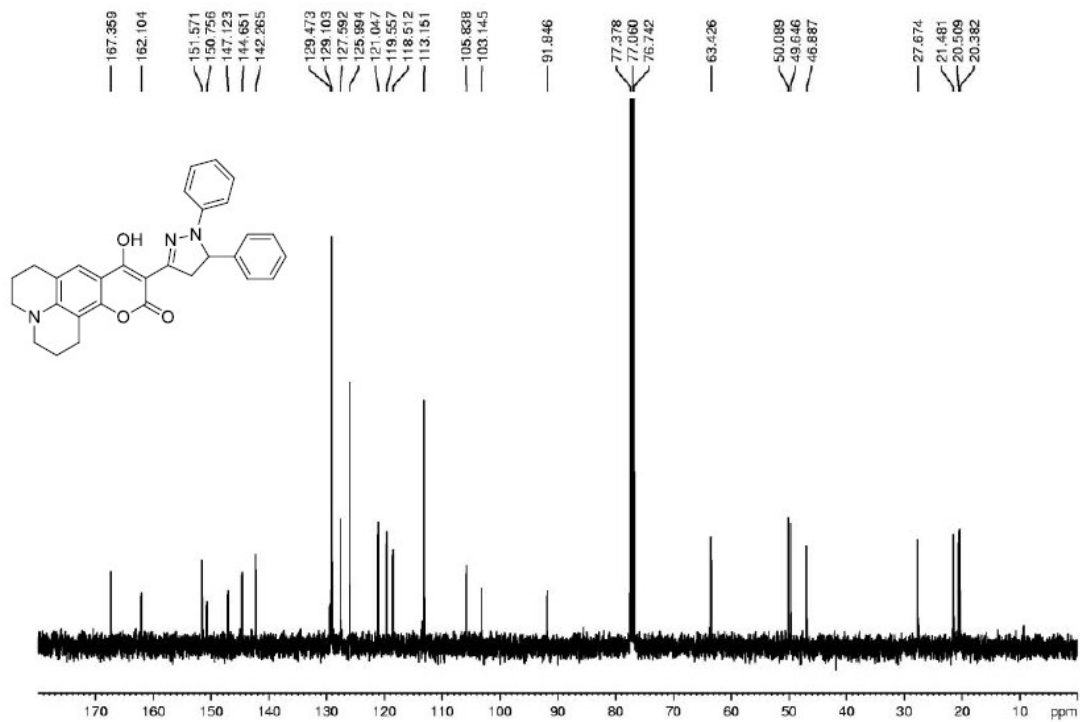


Fig. S2 Structure characterization of compound 3

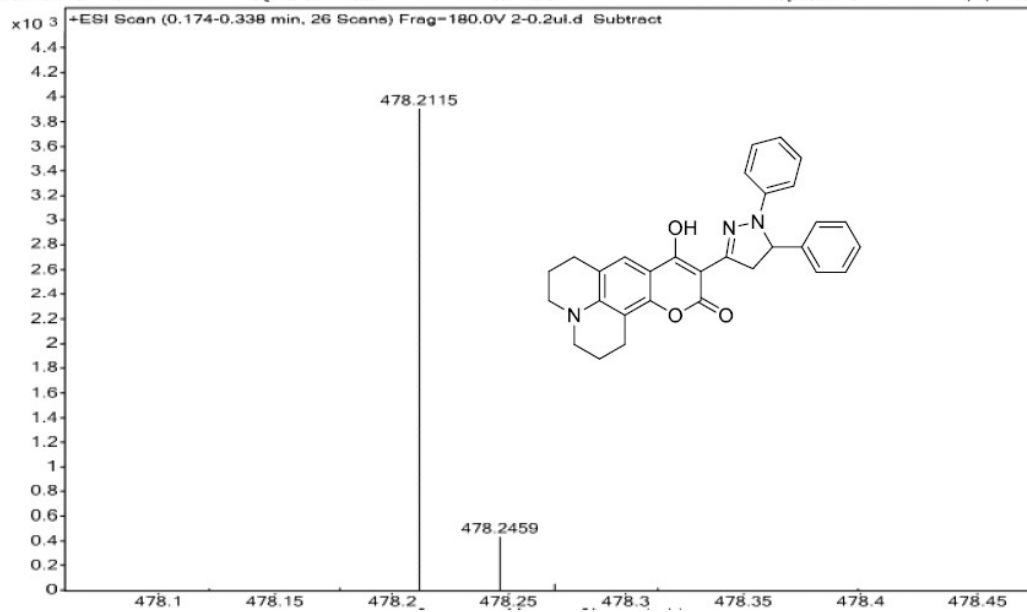


¹H-NMR spectrum of compound 3 in CDCl₃



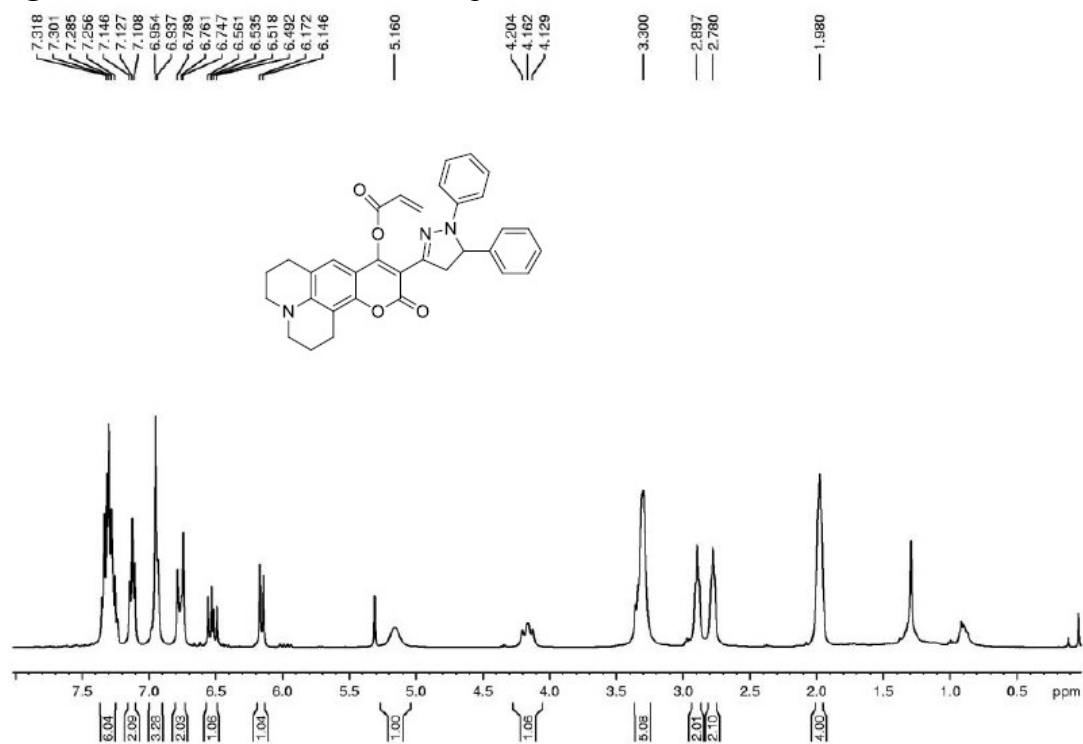
¹³C-NMR spectrum of compound 3 in CDCl₃

Sample Name	2	Position	P1-C2	Instrument Name	Instrument 1	User Name	Agilent FSE
Inj Vol	0.02	InjPosition		SampleType	Sample	IRM Calibration Status	Success
Data Filename	2-0.2u.d	ACQ Method	test.m	Comment		Acquired Time	9/12/17 Tue 16:27:33

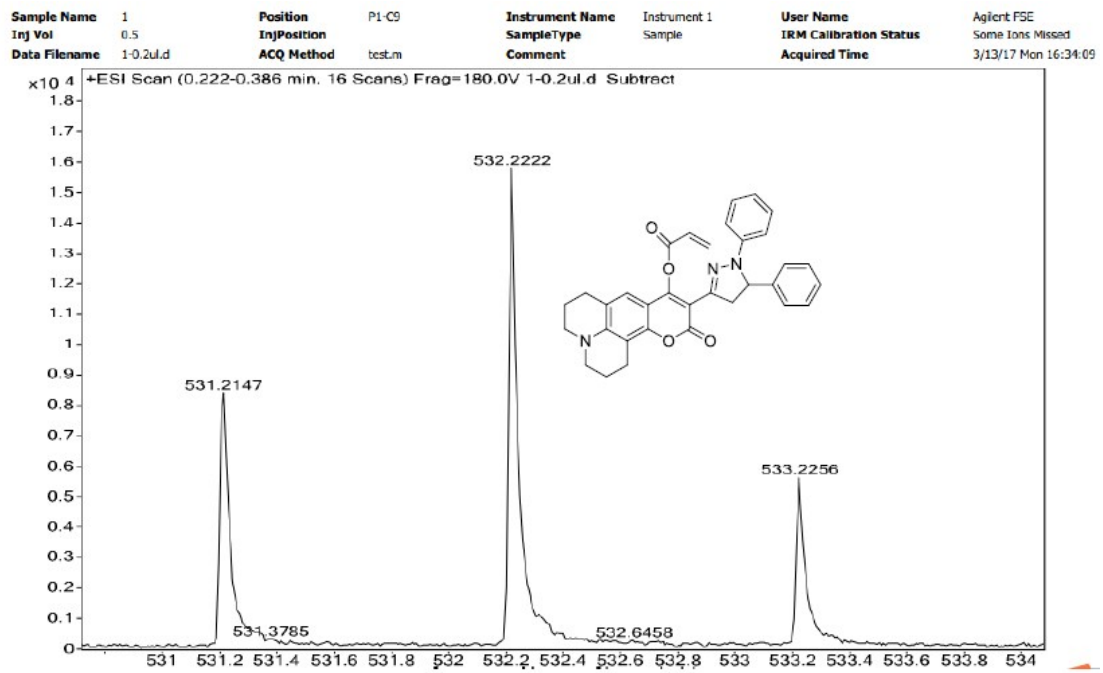
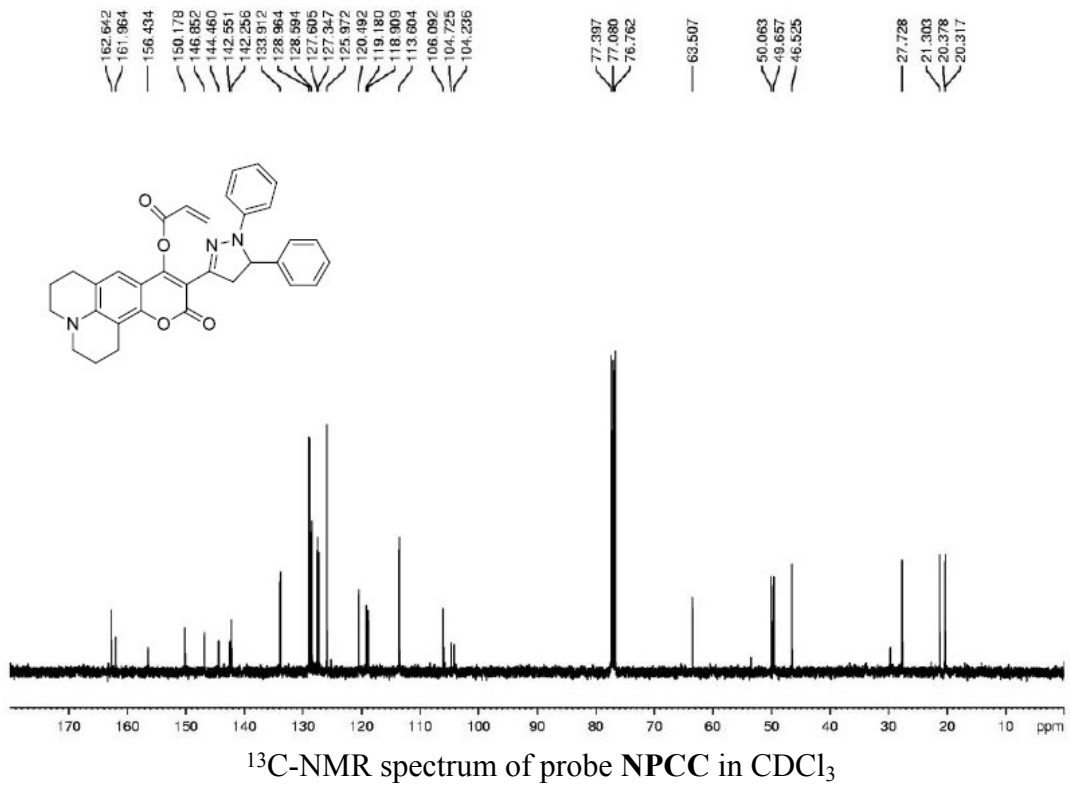


HR-MS spectrum of compound 3

Fig. S3 Structure characterization of probe NPCC



¹H-NMR spectrum of probe NPCC in CDCl₃



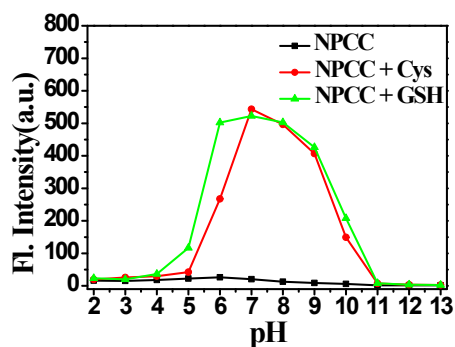


Fig. S4 The relationship between the emission intensity of NPCC and different pH medium before or after treated with 10 equiv. of Cys (red circle) or GSH (green triangle). Conditions: $\lambda_{\text{ex}} = 441 \text{ nm}$, $\lambda_{\text{em}} = 514 \text{ nm}$. Slit: 10/10 nm.

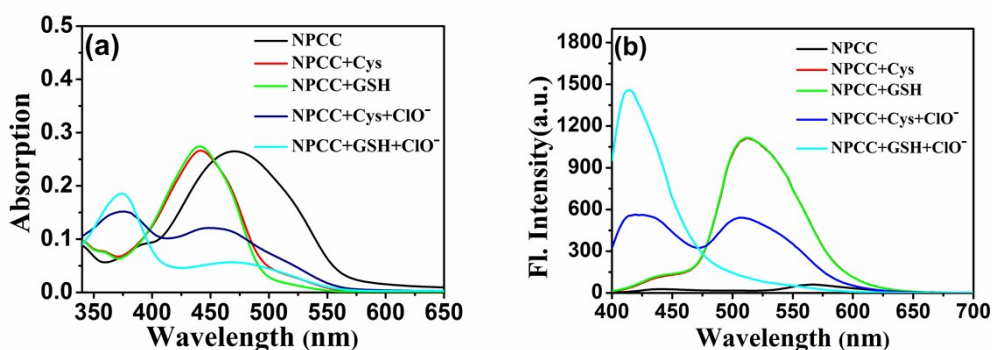


Fig. S5 The changes of (a) absorption and (b) emission spectral of NPCC (10 μM) in Tris-HCl buffer (10 mM, pH 7.4, with 1% CTAB).

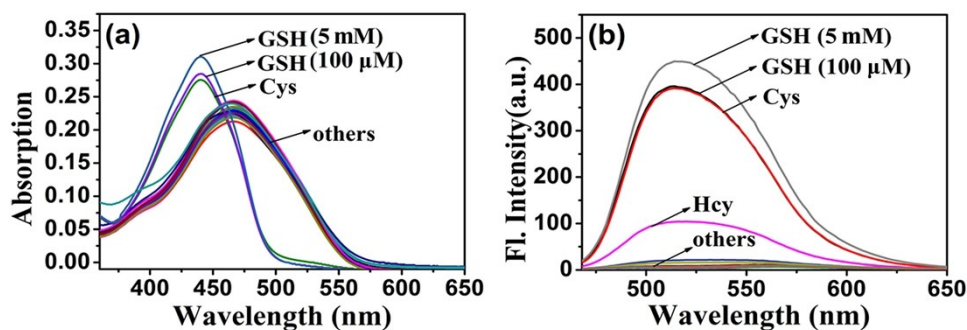


Fig. S6 (a) Absorption and (b) emission spectra of NPCC (10 μM) toward Cys (100 μM), GSH (100 μM and 5 mM) and other respective species (100 μM of Hcy, His, Glu, Asp, Val, Phe, Tyr, Ala, Ser, Leu, Arg, Pro, Thy, Lys, Gly, Na^+ , K^+ , F^- , Cl^- , Br^- , I^- , CO_3^{2-} , HCO_3^- , Ac^- , SO_4^{2-} , PO_4^{3-} , HSO_3^- , HS^- , NO_3^- , NO_2^- , $\bullet\text{OH}$, $\text{O}_2\bullet^-$, ClO^- and H_2O_2).

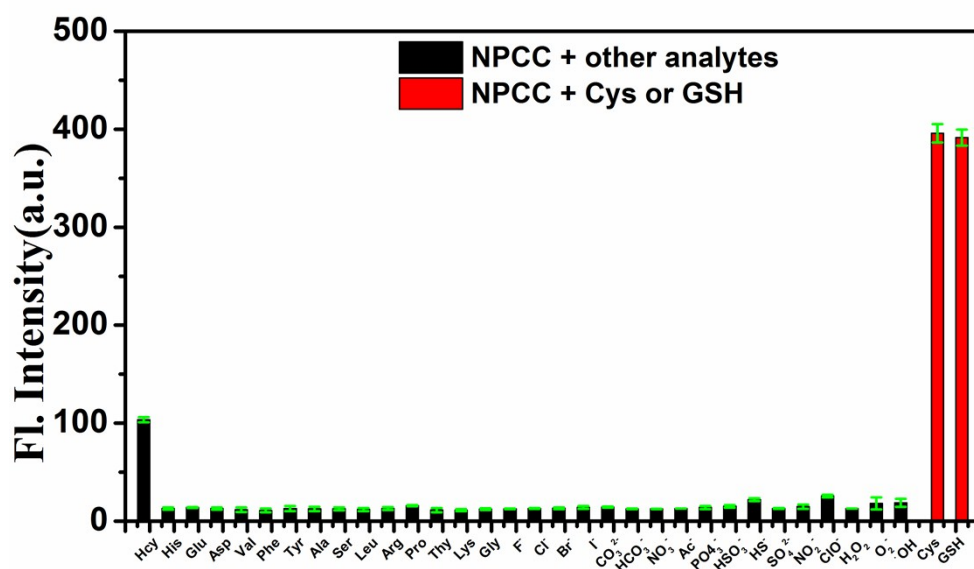


Fig. S7 Fluorescence spectra of NPCC (10 μ M) toward Cys, GSH (100 μ M) and other analytes (100 μ M of Hcy, His, Glu, Asp, Val, Phe, Tyr, Ala, Ser, Leu, Arg, Pro, Thy, Lys, Gly, Na⁺, K⁺, F⁻, Cl⁻, Br⁻, I⁻, CO₃²⁻, HCO₃⁻, Ac⁻, SO₄²⁻, PO₄³⁻, HSO₃⁻, HS⁻, NO₃⁻, NO₂⁻, \cdot OH, O₂⁻, ClO⁻ and H₂O₂). Conditions: λ_{ex} = 441 nm, λ_{em} = 514 nm. Slit: 10/10 nm.

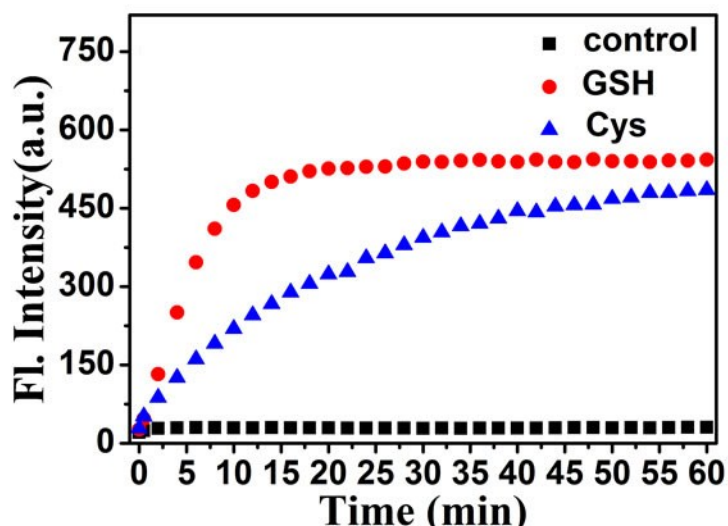


Fig. S8 Time-dependent fluorescence of NPCC before and after treated with 10 equiv. of Cys or GSH. Conditions: λ_{ex} = 441 nm, λ_{em} = 514 nm. Slit: 10/10 nm.

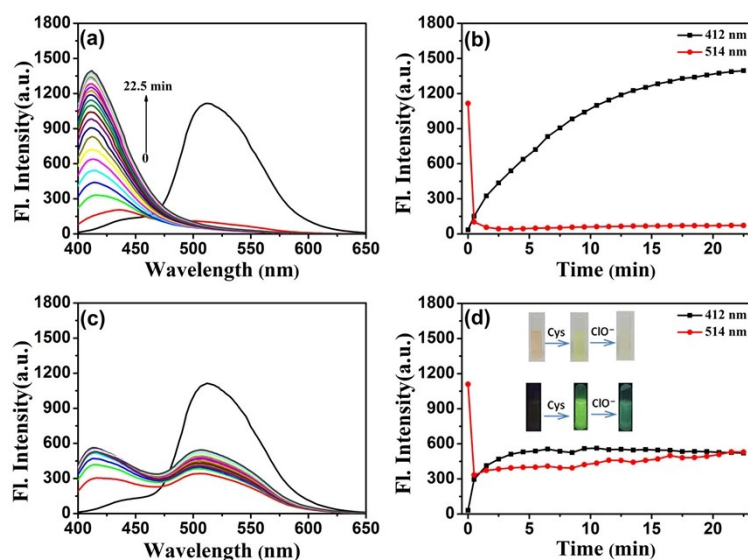


Fig. S9 Emission changes of NPCC (10 μM) with 10 equiv. of GSH (a and b) and Cys (c and d) at the prescribed time (0–22.5 min). Conditions: $\lambda_{\text{ex}} = 380 \text{ nm}$. Slit: 10/10 nm.

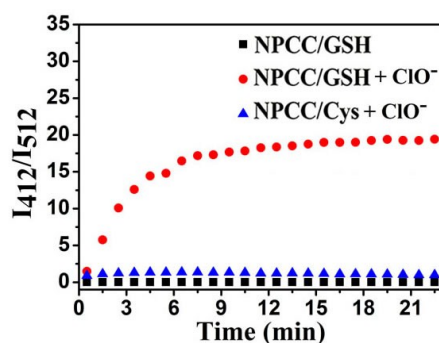


Fig. S10 Time-dependent fluorescence of NPCC/Cys and NPCC/GSH before and after treated with 30 equiv. of ClO⁻. Conditions: $\lambda_{\text{ex}} = 380 \text{ nm}$, $\lambda_{\text{em}} = 412 \text{ nm}$. Slit: 10/10 nm.

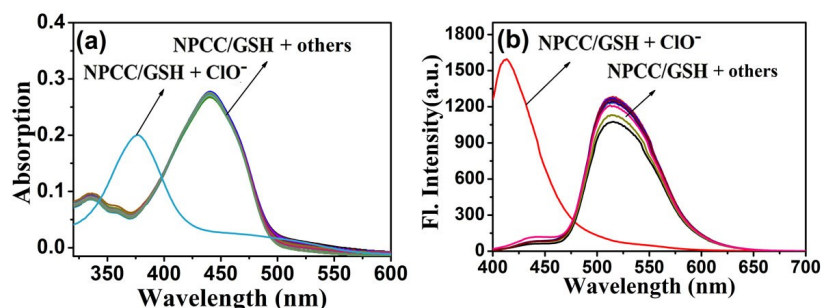


Fig. S11 (a) Absorption and (b) emission spectra of NPCC/GSH toward 300 μM of ClO⁻ and other analytes (Na⁺, K⁺, F⁻, Cl⁻, Br⁻, I⁻, CO₃²⁻, HCO₃⁻, Ac⁻, SO₄³⁻, S₂O₈²⁻, PO₄³⁻, ClO₄⁻, HSO₃⁻, HS⁻, NO₃⁻, •OH, NO₂⁻, ¹O₂, O₂•⁻ and H₂O₂).

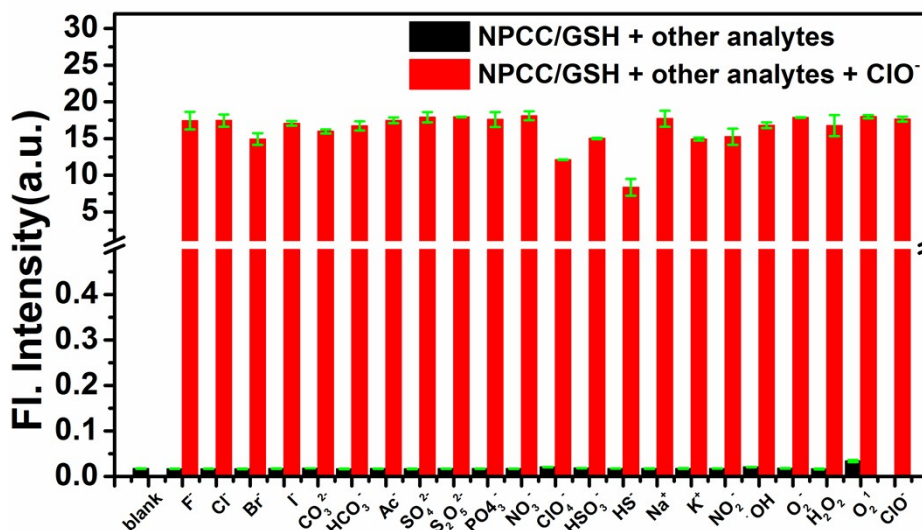


Fig. S12 The emission ratio (I_{412}/I_{514}) of NPCC/GSH toward different 30 equiv. of analytes. Black bars: NPCC/GSH toward different 30 equiv. of analytes, respectively. Red bars: NPCC/GSH at I_{412}/I_{514} in the copresence of ClO⁻ (300 μM) and other analytes (300 μM of Na⁺, K⁺, F⁻, Cl⁻, Br⁻, I⁻, CO₃²⁻, HCO₃⁻, Ac⁻, SO₄³⁻, S₂O₈²⁻, PO₄³⁻, ClO₄⁻, HSO₃⁻, HS⁻, NO₃⁻, •OH, NO₂⁻, ¹O₂, O₂•⁻ and H₂O₂), respectively. Conditions: $\lambda_{\text{ex}} = 380 \text{ nm}$, $\lambda_{\text{em}} = 412 \text{ nm}$. Slit: 10/10 nm.

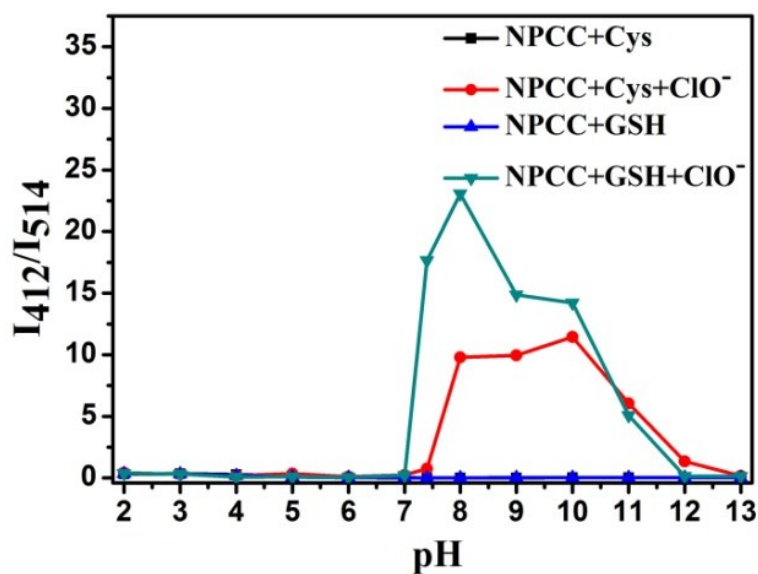
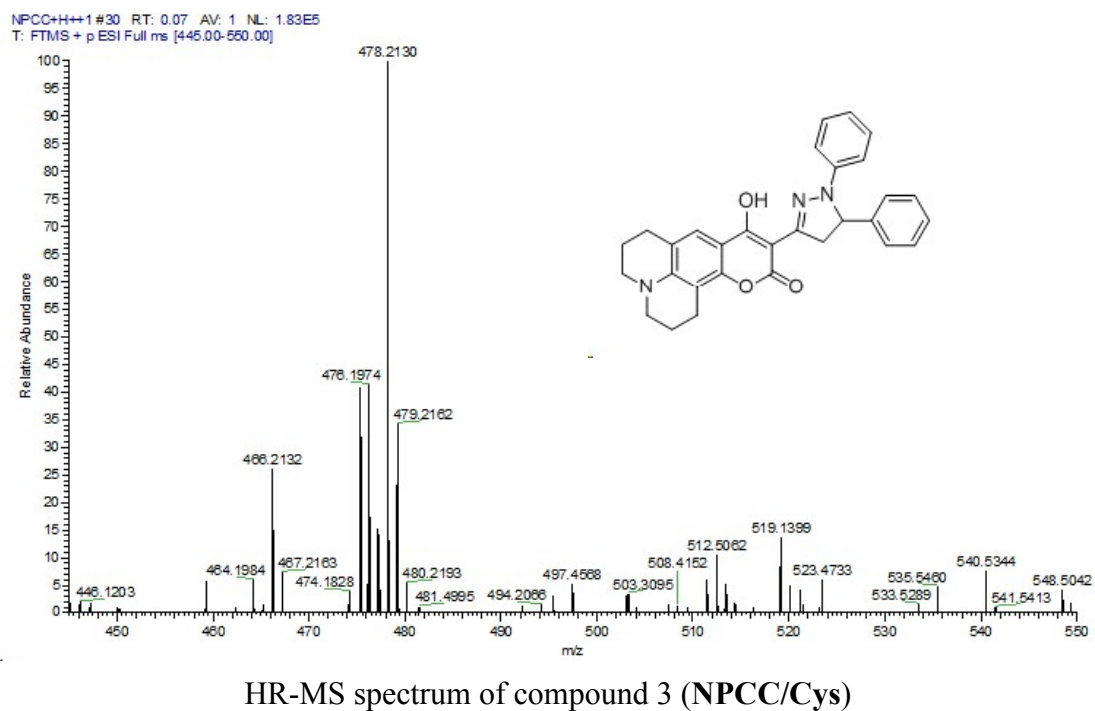
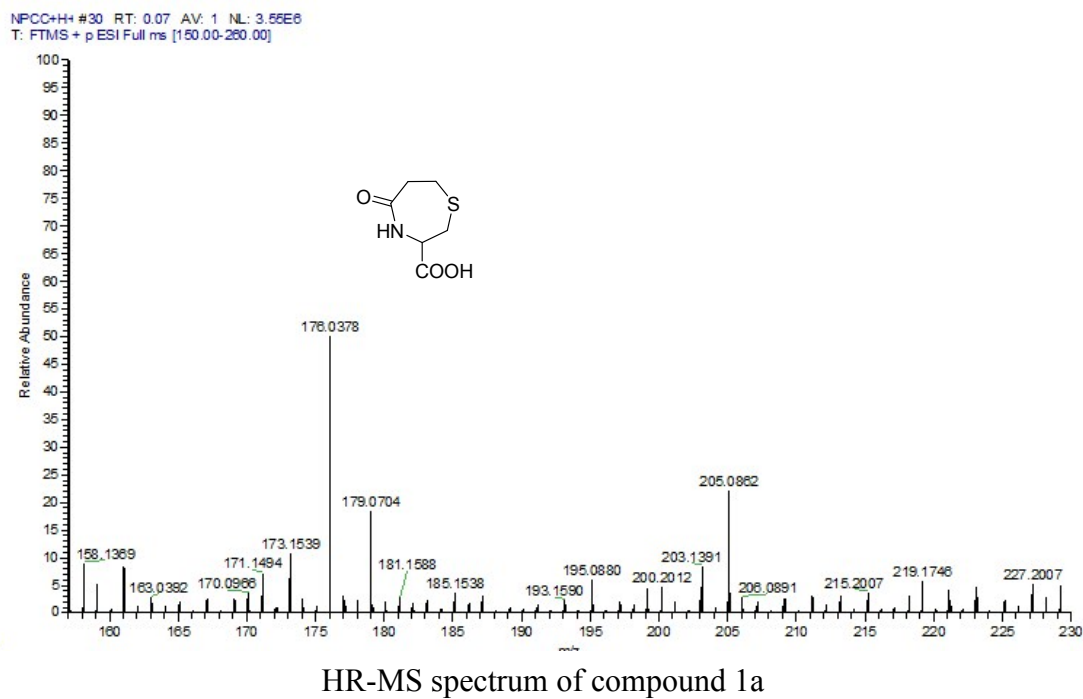
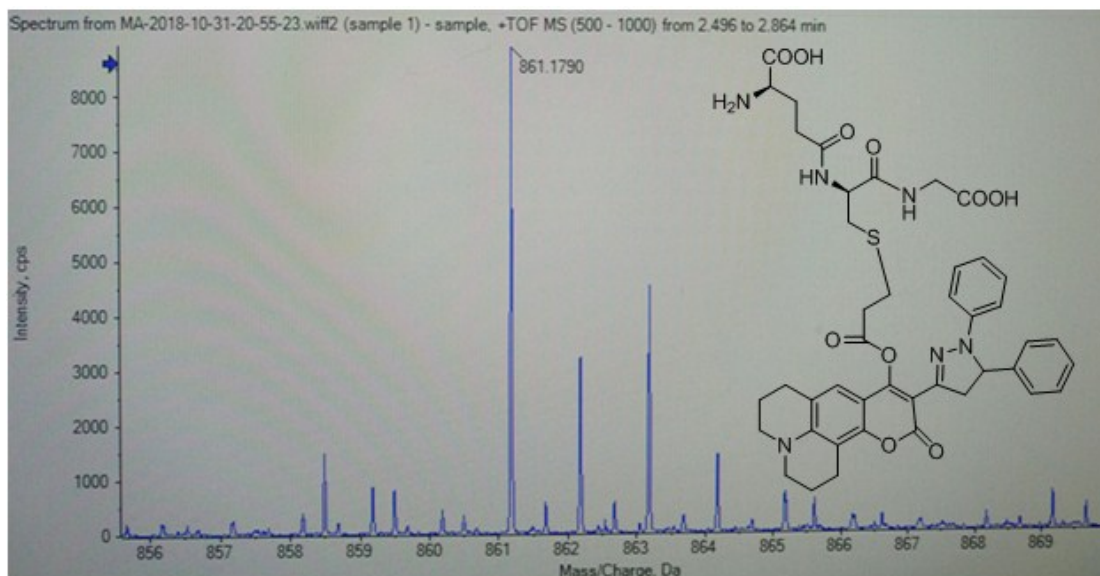


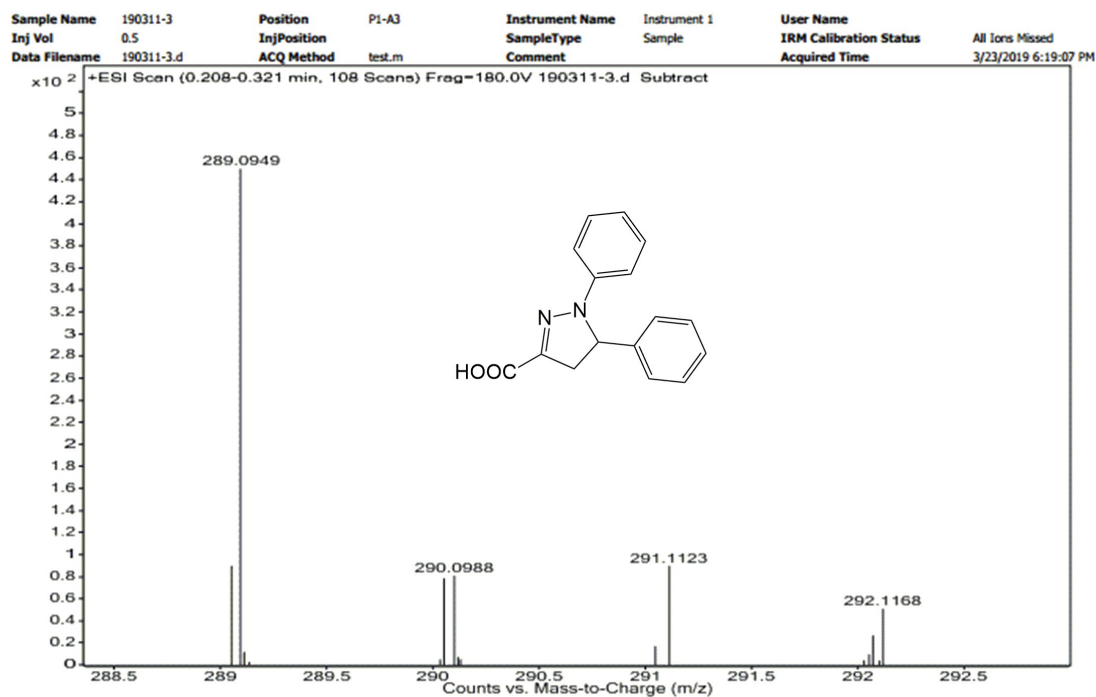
Fig. S13 The changes of the emission ratio (I_{412}/I_{514}) of NPCC/Cys and NPCC/GSH in different pH (range from 2.0 to 13.0) in Tris-HCl buffer (10 mM, with 1% CTAB). Incubation time: 15 min. Excitation: 380 nm. Slit: 10/10 nm.

Fig. S14 Sensing mechanism of NPCC toward Cys, GSH and ClO⁻.





HR-MS spectrum of NPCC/GSH



HR-MS spectrum of compound 1b

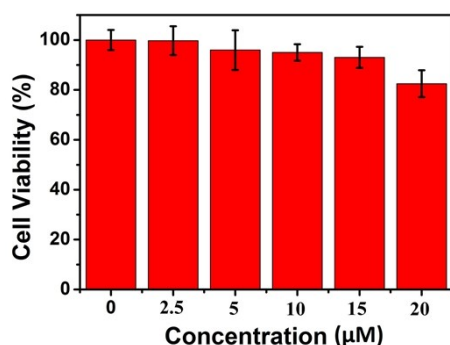


Fig. S15 Different NPCC concentrations (0, 2.5 μM, 5 μM, 10 μM, 15 μM, and 20 μM) were tested in EC1 cells for toxicity.

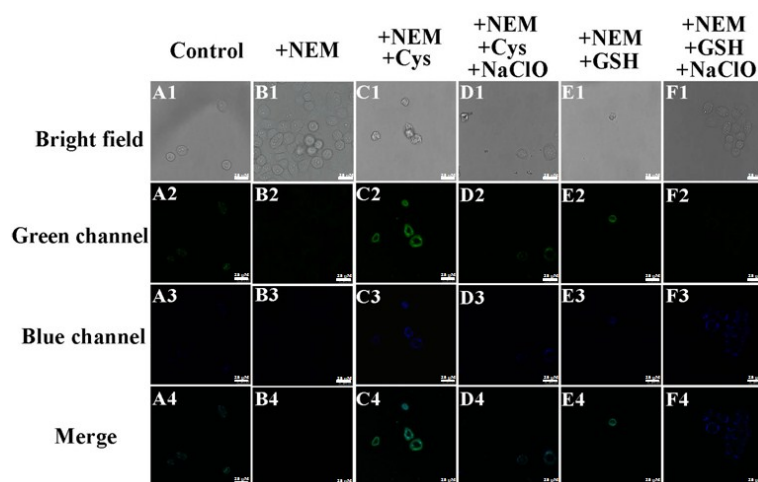


Fig. S16 Imaging of NPCC for detecting endogenous and exogenous Cys, GSH and ClO⁻ in EC1 cells. (A) NPCC was incubated with EC1 cells for 0.5 h. (B) EC1 cells were treated with 1 mM NEM for 0.5 h, and then NPCC was added for 0.5 h. (C) Cells were pretreated with 1 mM NEM for 0.5 h, and Cys (100 μM) were added, then NPCC was added for 0.5 h; (D) EC1 cells were pretreated with 1 mM NEM for 0.5 h, and Cys (100 μM) was added, then NPCC was added for 0.5 h, and finally incubated with ClO⁻ (300 μM) for 0.5 h; (E) Similar to C, Cys was replaced by GSH (100 μM); (F) Similar to D, Cys was replaced by GSH (100 μM). Conditions: for green channel, λ_{ex}= 440 nm, λ_{em}= 492–532 nm; for blue channel, λ_{ex}= 380 nm, λ_{em}= 392–432 nm. Scale bar: 25 μm.

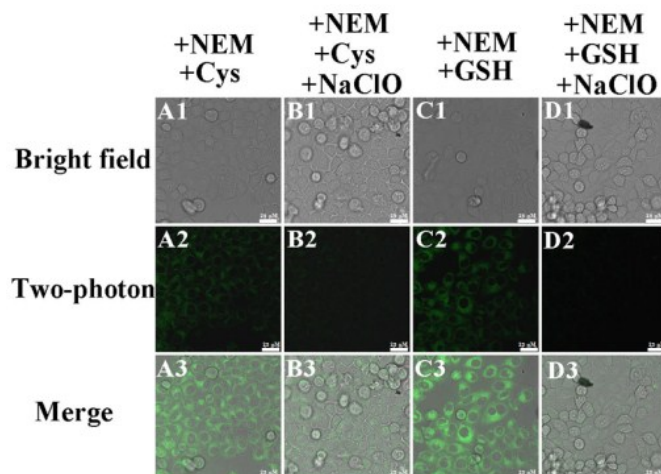


Fig. S17 TP imaging of Cys, GSH and ClO⁻ in EC1 cells. (A) EC1 cells were treated with 1 mM NEM for 0.5 h, and Cys (100 μM) were added for 0.5 h. (B) EC1 cells were pretreated with 1 mM NEM for 0.5 h, and Cys (100 μM) was added, then NPCC (10 μM) was added for 0.5 h, and finally incubated with ClO⁻ (300 μM) for 0.5 h. (C) Similar to A, Cys was replaced by GSH (100 μM); (D) Similar to B, Cys was replaced by GSH (100 μM). $\lambda_{\text{ex}} = 850 \text{ nm}$, $\lambda_{\text{em}} = 492\text{--}532 \text{ nm}$. Scale bar: 25 μm.

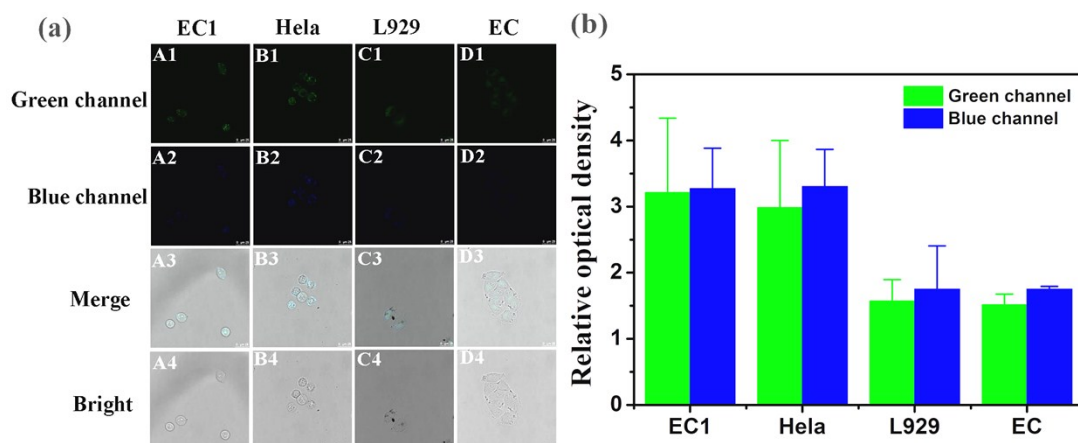


Fig. S18 Imaging of cancer cells and normal cells. NPCC were incubated with cancer cells (EC1 cells and HeLa cells) and normal cells (L929 cells and EC) for 0.5 h, respectively. Conditions: for green channel, $\lambda_{\text{ex}} = 440 \text{ nm}$, $\lambda_{\text{em}} = 492\text{--}532 \text{ nm}$; for blue channel, $\lambda_{\text{ex}} = 380 \text{ nm}$, $\lambda_{\text{em}} = 392\text{--}432 \text{ nm}$. Scale bar: 25 μm.